Extensive Air Showers Measured by the 79-string IceCube Observatory at South Pole

THE ICECUBE COLLABORATION[1]
[1] *See special section in these proceedings*

Abstract: The IceCube Neutrino Observatory was completed in the 2010-11 Antarctic season with 86 deep strings and 81 surface stations. Between June 2010 and May 2011 IceCube collected high quality data with 73 stations and 79 strings. The performance of the detector as an air shower array to contribute to our understanding of the cosmic ray spectrum from the knee region up to 1 EeV will be demonstrated. The sensitivity to primary composition using high energy muon bundles seen by the IceCube array will also be discussed.

Corresponding authors: T. Feusels[2] (*tom.feusels@ugent.be*), S. Tilav[3] (*tilav@udel.edu*)
[2]*Dept. of Physics and Astronomy, University of Gent, B-9000 Gent, Belgium*
[3]*Bartol Research Institute and Dept. of Physics and Astronomy, University of Delaware, Newark, DE 19716, U.S.A.*

Keywords: IceTop; IceCube; Extensive Air showers; Muon bundles

DOI: 10.7529/ICRC2011/V01/0838

1 Introduction

The IceCube Neutrino Observatory started taking data in May 2011 with the complete array of 81 surface stations and 86 strings in the deep Antarctic ice [1]. The array grid is shown in Figure 1. In the period of June 2010-May 2011, the surface air shower array, IceTop [2], was operated with 73 stations (146 ice Cherenkov tanks) positioned on a triangular grid with a 125 m spacing. The IceCube detector had 79 strings with 60 sensors on each string at depths between 1450 m and 2450 m in the ice. We refer to this configuration as IceTop-73/IceCube-79. The detector collected data with 98% uptime during this period.

IceCube, located at the geographic South Pole (altitude: 2835 m), is at an optimum atmospheric depth of 680 g/cm^2 where cosmic ray air showers in the PeV energy range are close to their shower maximum. In addition, with fast digital electronics for signal processing and high resolution waveforms, IceTop is in a unique position to make a detailed measurement of the cosmic ray energy spectrum in this energy region in a few years. About 30% of showers trigger both detectors; these are called coincident events. The energy deposited along the kilometer long tracks of the penetrating muon bundles in IceCube, when combined with the energy deposited on the surface in IceTop, provide a mass composition sensitive measurement.

In this paper we evaluate the performance of IceCube as a three dimensional Extensive Air Shower (EAS) array based on nine months of data from June 15, 2010 to March 15, 2011. The data is split into an austral winter dataset (Jun 15, 2010 - Nov 1, 2010) and an austral summer dataset

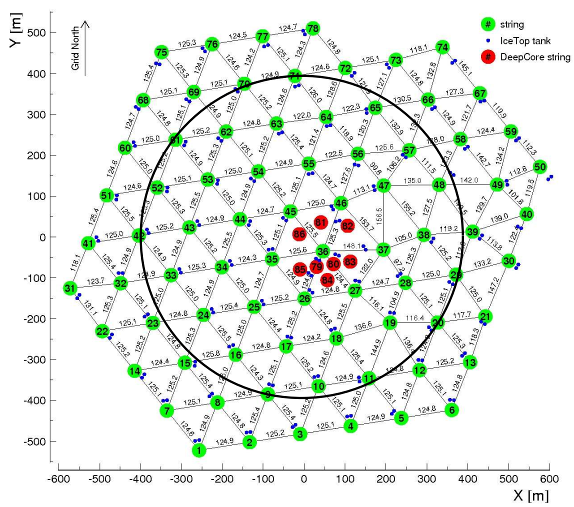

Figure 1: The surface map of IceCube in its completed configuration. IceTop Stations 1, 7, 14, 22, 31, 79, 80 and 81 were not yet deployed in 2010. The circle with a 400 m radius shows the containment criterium for the reconstructed shower core position.

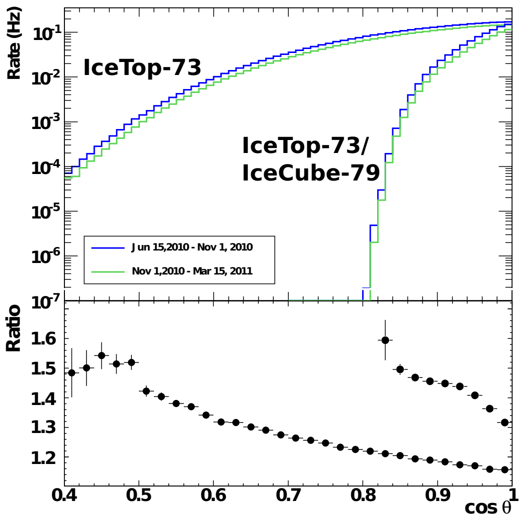

Figure 2: The differential rate of events in cosine zenith angle is shown in the top plot for IceTop-73 data and for coincident data. The dark (blue) and light (green) lines represent the austral winter and summer rates respectively. The ratio of winter to summer rates in the bottom plot shows the zenith angle dependence.

(Nov 1, 2010 - Mar 15, 2011) to investigate the basic shower observables and their temporal behaviour due to atmospheric changes. After minimal cuts the quality of the reconstructed events already reaches an accuracy to probe the inherent systematics left in data which may degrade the energy resolution and thus need to be studied further.

This analysis uses the largest statistical data set which covers two austral seasonal conditions. Earlier analyses [3, 4] did not account for atmospheric changes and could therefore not combine data of more than one season.

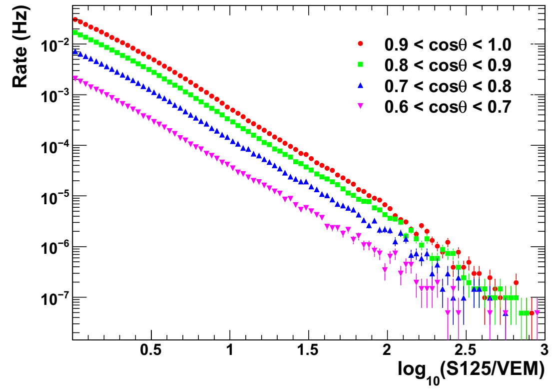

Figure 3: The differential rate of $\log_{10}(S_{125})$ for four zenith angle bands of equal solid angle in the region where IceTop is fully efficient. The plot quantifies the attenuation of showers with zenith angle. This attenuation is corrected when converting S_{125} to primary energy.

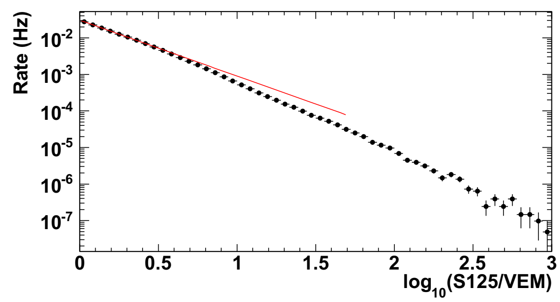

Figure 4: The differential rate of $\log_{10}(S_{125})$ for the coincident IceTop-73/IceCube-79 events with a line fitted between 0 and 0.5 to guide the eye.

2 Reconstruction of basic observables

IceTop measures the Cherenkov light emitted by charged particles passing through the tanks. The timing information is used to reconstruct the arrival direction, while the signal strength is used for the core position. The lateral distribution of the energy deposition by each shower is fitted to a function of the signal strength in Vertical Equivalent Muons (VEM) versus distance to shower core. The signal strength evaluated at 125 m from the reconstructed shower core, S_{125}, is found by simulation studies to be sufficiently mass independent to primary energy for nearly vertical showers [5]. For coincident events also the IceCube signals were used, together with a fixed reconstructed core position at the surface, to fit the direction using a function which describes the muon bundle range-out [4]. This improves the angular resolution [6] and will be used to remove unrelated IceTop/IceCube coincident events.

2.1 Event selection

Air shower events which trigger at least five IceTop stations were reconstructed with the standard IceTop reconstruction procedure [7]. The events were selected if the reconstructed observables converged successfully, and the core location was reconstructed within a circle of 400 m radius from the IceTop array center as shown in Figure 1. On average, the reconstructed event rate was 2.55 Hz with a 12% variability due to the barometric pressure changes.

Events which trigger both the IceTop and the IceCube array, but do not belong to the same air shower constitute an important background for the coincident data sample. These so-called random coincident events were cut based on the time difference between the signals in IceTop and the signals in IceCube. The zenith angle difference between IceTop and IceCube direction reconstructions was also used to remove random coincident events. For a good energy loss reconstruction in the deep ice, the muon tracks which were not well contained by the detector volume (corner clippers) were not used in the final sample. This basic

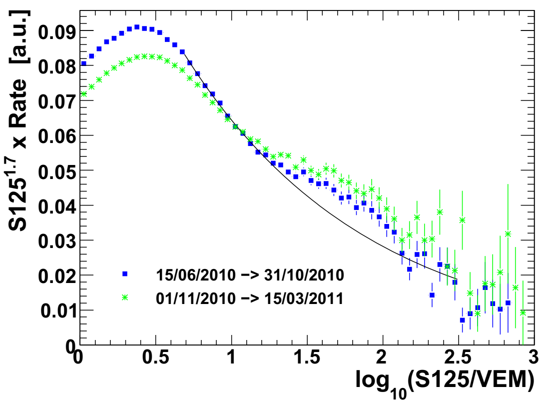

Figure 5: The weighted spectrum of $\log_{10}(S_{125})$ for the IceTop-73 events with $\cos\theta > 0.8$ is shown for winter and summer months by (blue) squares and (green) stars respectively. An exponential function is fitted to the slope of the winter curve between 0.7 and 1.1 and extrapolated to $\log_{10}(S_{125}) = 2.5$ to guide the eye.

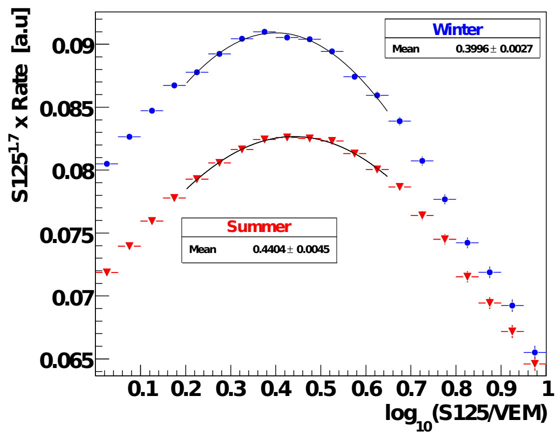

Figure 6: The knee region of the S_{125} spectrum. A shift of 0.04 in $\log_{10}(S_{125})$ is observed between the winter (blue circles) and summer (red triangles) spectra.

set of cuts results in a high quality, well reconstructed data sample with an angular resolution below 1° and a core resolution of about 10 m. The average IceTop-73/IceCube-79 coincident event rate after this selection was 0.72 Hz with a 15% variability.

In total 34.8 million events were left in the IceTop-73 data sample, while 9.5 million events remained in the coincident data sample (for a livetime of 236.44 days).

2.2 Basic shower observables and their temporal behaviour

Figure 2 shows the differential rate in cosine zenith angle for both IceTop-73 events and IceTop-73/IceCube-79 coincident events. The requirement that the muon bundle component of the air shower must pass through the IceCube detector leads to a steeper distribution for the coincident events. The light (green) line is the rate in the austral summer season and the dark (blue) line shows the rate in the austral winter season. The change in the atmospheric density profile [8] from winter to summer as well as the snow accumulation of 21 cm on average during 2010 contribute to the observed difference in rates between the two seasons. The ratio quantifies the angular dependence of both atmospheric and snow effects.

The differential rate of $\log_{10}(S_{125})$ is plotted for four zenith angle bands of equal solid angle in Figure 3 in the range where IceTop is fully efficient. The rate difference observed between the different zenith bands is due to the atmospheric attenuation. We could apply the classic Constant Intensity Cut analysis by calculating the attenuation for different zenith angles and evaluating the spectra at one zenith angle. In this analysis the IceTop-73 events were restricted to $\cos\theta > 0.8$ to study the atmospheric effects within this narrow angular range. However, with high statistics it will be possible to use each zenith band as a separate dataset to reconstruct and analyze with different methods and further explore its mass composition sensitivity.

In Figure 4 the differential rates of $\log_{10}(S_{125})$ for the coincident IceTop-73/IceCube-79 events are presented. The break seen in slope of the spectra around $\log_{10}(S_{125}) = 0.4$ is the cosmic ray knee.

To probe the details in the spectrum the rate weighted by $S_{125}^{1.7}$ for $\cos\theta > 0.8$ is plotted in Figure 5. It is interesting to note the opposite behaviour of the high and low energy events in different atmospheric conditions, causing a change in the slope. The spectra show a hardening trend between $1.2 < \log_{10}(S_{125}) < 2.1$. This systematically significant feature could not be traced back to any anomaly in data and is also seen by previous analyses [3, 4].

The knee position changes by 0.04 in $\log_{10}(S_{125})$, from 0.44 in summer to 0.40 in winter as shown in Figure 6. As the knee position should be at the same primary energy, the conversion from S_{125} to primary energy will need to take into account that the atmospheric variation and snow accumulation changes the detector response for the same primary energies.

From an energy estimator, which was derived by simulations of proton showers, $\log_{10}(S_{125}) = 1$ corresponds to about 10 PeV, $\log_{10}(S_{125}) = 2$ to about 100 PeV, and $\log_{10}(S_{125}) = 2.7$ to about 1 EeV. From Figures 3 and 4, the measured rates indicate that about 150 events per year are measured by the three dimensional IceCube air shower array above 300 PeV and about 15 events above 1 EeV. There is also no indication of array saturation up to 1 EeV.

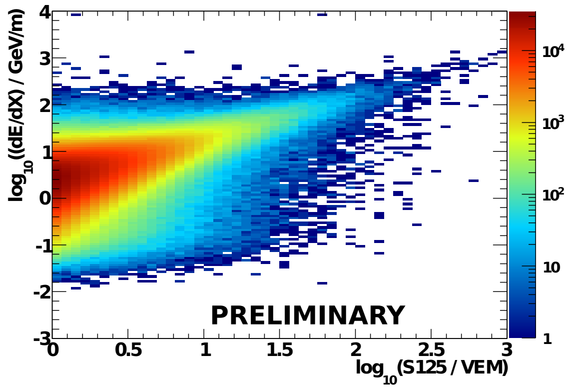

Figure 7: The average muon bundle energy loss $\frac{dE}{dX}$, measured by IceCube, shows a strong correlation with the shower size, reconstructed by IceTop, up to the highest cosmic ray energies.

3 Sensitivity to primary composition

When EAS propagate through the South Pole ice layer, only narrow ($\sim$ 20 m) bundles of highly energetic muons (>500 GeV) survive to the depth of IceCube. They will lose energy mainly stochastically which then generates Cherenkov light detected by IceCube. Here the average energy loss of muon bundles at the center of the IceCube detector volume is reconstructed using the measured charge signals and taking into account light propagation and the ice properties [9]. The energy loss of a muon bundle is a convolution of the muon multiplicity, the muon energy distribution within the bundle and the single muon energy loss. Both the multiplicity and the energy distribution depend highly on the primary mass and energy. Thus, the muon bundle energy loss provides a composition sensitive observable and can be determined with a resolution of about 0.3 in $\log_{10}$ of $\frac{dE}{dX}$ [9].

In Figure 7, nine months of high quality coincident data is shown. There is a clear correlation between the IceTop energy sensitive observable, S_{125}, and the energy loss up to the highest energies. Also, the shape of the distribution becomes narrower for higher S_{125} (larger showers). From simulations we know that proton and iron distributions become well separated in energy loss as function of primary energy [6]. The narrower distribution could therefore be related to a change in composition and will be studied further by simulations.

Events with a relatively low energy deposition in IceCube and no correlation with the IceTop shower size form the main background at this basic level of cuts as these are mainly caused by remaining random coincident events. However with minor cuts this is already reduced to the $\sim$1% level and will be further reduced in the next stage of the analysis.

4 Summary/Outlook

In this paper the performance of IceCube as a three dimensional cosmic ray detector was investigated using nine months of high quality data from June 15, 2010 to March 15, 2011 when the IceCube detector was in its 73-station/79-string configuration. We studied the behaviour of the basic observables in two distinct atmospheric conditions with the data split as austral winter and summer sets. We observed the change induced on the lateral development of showers by the atmospheric effects and snow accumulation, and a shift of 0.04 in $\log_{10}(S_{125})$ around the cosmic ray knee region between the two datasets. This observable effect on the shower development will be studied in detail. We observed that the high and low energy showers are affected by the seasonal effects in opposite way, having a higher rate of high energy showers in the austral summer atmosphere than in winter. The S_{125} spectra shows a systematically significant hardening between $1.2 < \log_{10}(S_{125}) < 2.1$. The cause of these effects, whether due to a change in shower maximum, change in the energy spectrum or a change in mass composition, will be the subject of further studies.

The observed zenith angle dependence of EAS and the seasonal expansion of the atmosphere can be used for composition studies. For coincident IceTop/IceCube air showers the composition sensitive ratio of muon bundle energy loss to shower size at the surface as well as the width of the energy loss distribution is being exploited.

A few years of cosmic ray data will already provide enough statistics to accurately measure cosmic ray energy spectrum and composition up to 1 EeV by using multiple composition and energy dependent shower observables through different techniques such as neural networks [4].

References

[1] H. Kolanoski, IceCube summary talk, these Proceedings.
[2] IceCube Collaboration, paper 807, these Proceedings.
[3] “All-particle cosmic ray energy spectrum measured with 26 IceTop stations” (The IceCube Collaboration), to be published.
[4] IceCube Collaboration, paper 923, these Proceedings.
[5] IceCube Collaboration, paper 379, these Proceedings.
[6] T. Feusels *et al.* , In Proc. 31th ICRC, Lodz, Poland, 2009, arXiv:0912.4668.
[7] S. Klepser, PhD thesis, Humboldt Univ, Berlin (2008).
[8] S. Tilav *et al.* , In Proc. 31th ICRC, Lodz, Poland, 2009, arXiv:1001.0776.
[9] S. Grullon *et al.* , In Proc. 30th ICRC, Merida, Mexico, 2007.